RESEARCH ARTICLE OPEN ACCESS

Structural, Optical, Antibacterial Activity of Undoped, Doped and Capped ZnO Nanoparticles Prepared by Simple Chemical Method towards Eco-friendly Synthesis

P Joseph Samrat[1], P S V Subba Rao[2]

1(Department of Physics, Brilliant Institute of Engineering & Technology, Hyderabad - 501 505, Telangana,India.)
2(Department of Physics, College of Science & Technology, Andhra University, Visakhapatnam -530 003, Andhra Pradesh, India.)

Abstract:

The zinc oxide (ZnO) nanoparticles were prepared by using simple chemical method which was in the form of undoped, doped and capped nanoparticles. Then their structural, morphological, optical properties were characterized by using X-ray diffraction (XRD), transmission electron microscopy (TEM), ultraviolet visible spectroscopy (UV) and photoluminescence spectroscopy (PL) techniques. The hexagonal crystal structure was observed from XRD patterns and their calculated crystallite sizes were approximately 15-20 nm. The spherical shaped particles nature was observed from TEM images. The FTIR spectrum confirms the Zn-O stretching mode. The optical absorption behavior was observed from UV spectrum which was blue-shifted behavior and their calculated bandgap energy value was approximately 3.8-3.7 eV. The emission behavior was observed from PL spectrum which was enhanced emission nature. Further, the antibacterial activity was measured on *E.coli*. Hence the observed results are discussed in detail.

Keywords — **ZnO Nanoparticles, doped, capped, Optical properties and Antibacterial activity.**

I. INTRODUCTION:

In the past and recent years, the semiconductor nanocrystals have drawn an enormous research attention because of their great potential in electronics, photonics, opto-electronics and bio-applications [1-4]. The optical properties strongly depend on the quantum size effects [5]. The ZnO is a versatile semiconductor with a wide bandgap of approximately 3.37 eV and their unique optical properties and biocompatibility nature shows huge advantages than metal as well as chalcogenide nanoparticles. Hence, some of the methods have been reported [6-7] the synthesis of ZnO nanocrystals in aqueous solution under room temperature but they all involved alkaline media or annealing conditions and therefore they are not exactly suitable for biological applications. In order to make ZnO nanocrystals for bio-applications, the synthesis process has to meet several requirements like, contain only bio-compatible materials or suitable surface capping ZnO particles in a stable colloidal solution [8]. Current drive is to integrate the "simple chemical method towards eco-friendly synthesis" like green synthesis approach which is used to design environmentally benign materials and processes. In recent years, it can be used as an environmental friendly system for the synthesis and stabilization of metal nanoparticles by suitable choice of materials and solvents suggested by some research reports [9-10]. The biomolecules serves as an environmentally benign reducing agent for the metal ions and starch also provides stable surface passivation or protection to prevent the aggregation of the particles. Hence, the "biomolecules based capping agent" is one of the best candidates to prepare nanomaterials [11]. Therefore, starch is selected as the protecting agent in the

present work because it is renewable and it can form dispersion in water. Similarly among the natural polymers, starch is one of the most promising bio-compatible and bio-degradable materials [12-14]. In general, bacteria perform many critical roles in the system function and productivity. The toxicity of nanoparticles (NPs) to bacteria has caused many concerns. Interactions between the bacteria and NPs may provide us with more information about the impact of NPs. This research is, therefore, performed to better understand whether the bacterial toxicity of NPs is size or composition related by comparing the NPs to their bulk counterparts. Some of the bacterial activities on NPs have been reported and their activities against both gram negative and gram positive bacteria in which ZnO NPs have been well known, studied in *Escherichia coli (E.coli)* [15-21].

In the present work, a simple chemical precipitation method was used for the synthesis of undoped ZnO, doped ZnO and capped ZnO nanoparticles. Further we have investigated the optical properties and antibacterial activities of NPs. Hence the observed results were discussed in details.

II. MATERIAL AND METHODS

A. Chemicals:

All chemicals used were standard analytical grade (AR) and not further treated. Zinc acetate ($Zn(CH_3COO)_2$), sodium hydroxide (NaOH), starch, peptone and agar are the precursors with the solvent of double distilled water (DDW). Gram negative *E.coli bacteria* were used for bacterial study.

B. Synthesis of Nanoparticles:

For the synthesis of undoped ZnO NPs, the freshly prepared 0.5 mole of $Zn(CH_3COO)_2$ solution was stirred well using magnetic stirrer. Then the NaOH (base solution) solution was slowly added dropwise into the zinc acetate solution till the pH becomes 10. The mixture was stirred vigorously and then the white color solution was obtained. Further, the solution was used to ultrasonic treatment for stabilization of particles. Finally, the solution was stored without any disturbance, and then the particles sedimentation was obtained. The sedimentation was washed several times to remove unreacted compounds. After centrifuge, the particles are separated from the solution and then dried. Further the sample was oxidized through the annealing treatment using muffle furnace. Finally, a white color ZnO powder was obtained.

For the synthesis of doped ZnO NPs, the freshly prepared 0.5 mole of $Zn(CH_3COO)_2$ solution was stirred well using magnetic stirrer and then 0.5 mole of dopant solution was added before adding the NaOH (base solution) solution into the zinc acetate solution. For the synthesis of capped ZnO NPs, the above mentioned same procedure was repeated. Here the capping agent of starch is used to cover the ZnO particles which were added dropwise into the zinc acetate solution before changing the pH value. Finally, the prepared samples are used for various characterization techniques.

C. Antibacterial activity test:

In the laboratory, the *E.coli* bacteria were grown at 37ºC in a Luria-Broth (LB) medium. For the mixture containing 1.5 g of beef extract, 2.5 g of peptone and the pH value was adjusted to 7 using NaOH. Further 10 g of agar was added to the above solution and then sterilized in autoclave. Finally, the nutrient agar medium was prepared and filled in petri-plates. The grown bacteria were sprayed evenly in the petri-plates using sterile glass rod and then allowed to dry. Hence before conducting the bacterial assay, a 5 mg of NPs powder samples were dispersed into 10 ml of DDW. Then the solution was allowed to ultrasonic treatment to get fine dispersed particles. Further the diluted NPs solutions are

added into the bacteria medium and then incubated.

D. Characterization techniques:

The prepared powder samples were used by the following characterization techniques. The X-ray diffraction (XRD) pattern was recorded to confirm the crystal structure using powder X-ray diffraction technique (X'pert PRO). The surface morphology was observed through transmission electron microscope (TEM) technique (JEM-2010). The presence of chemical structure and functional groups were confirmed using Fourier infrared transform spectrometer (FTIR, Brucker-Tensor 27). The absorption spectrum was recorded using UV-VIS-NIR spectrophotometer (Shimatz-3600) to find out the bandgap energy. The photoluminescence (PL) emission behaviors were measured using spectrofluorometer (Specrofluoromax-4).

III. RESULTS AND DISCUSSION:

A. XRD - Structural analysis:-

Figure 1 shows the XRD patterns of (a) undoped ZnO, (b) doped ZnO and (c) capped ZnO NPs. All the samples indicate a hexagonal (wurtzite) crystal structure and it is in close agreement with the standard values (JCPDS card: 36-1451). The Debye-Sherrer's formula was used to calculate the crystallite sizes (D) and their calculated sizes were 15-20 nm.

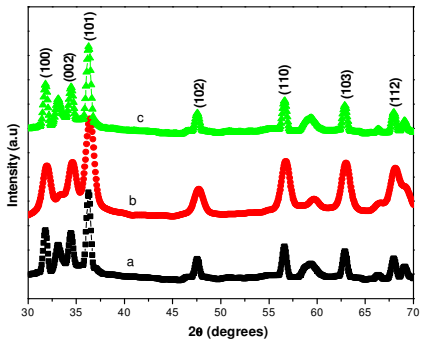

Figure 1. XRD pattern of (a) ZnO NPs, (b) ZnO:Fe NPs and (c) capped ZnO NPs

There was no phase changes observed for starch capped ZnO NPs due to the encapsulation effect because of its chemical composition. However a small variation in the peak broadening and intensity was observed in both the doped and capped ZnO NPs.

B. TEM - Morphology analysis:-

Figure 2 shows TEM images of (a) undoped ZnO, (b) doped ZnO and (c) capped ZnO NPs. The powder samples embedded on copper coated grid shows spherical nature and its sizes were around 15-20 nm for undoped and doped ZnO NPs. From the capped ZnO NPs, the aggregation occurred due to the polymer like medium and shows agglomerated spherical shaped particles. This morphology clearly shows the monodispersed nanoparticles due to the effect of starch on ZnO crystal. This type of morphology was observed earlier in starch capped CdSe nanostructures [22]. Therefore, the calculation of particle size is difficult due to agglomeration of particle but it may be approximately 15-20 nm.

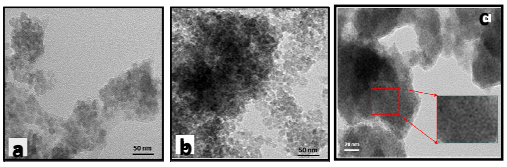

Figure 2. TEM image of (a) ZnO NPs, (b) ZnO:Fe NPs and (c) capped ZnO NPs

C. FTIR – Functional group analysis:-

Figure 3 shows FTIR spectrum of (a) undoped ZnO, (b) doped ZnO and (c) capped ZnO NPs. The band located between 400-550 cm^{-1} was attributed due to Zn-O stretching mode. The other bands are corresponding to the stretching vibration of –OH bond and 1410 cm^{-1} was due to asymmetric and symmetric stretching vibration of carbonyl group which was known as COO-Zn coordination. The peaks at 1150 cm^{-1} and

1080 cm^{-1} was due to the anhydroglucose ring of starch and 2930 cm^{-1} was characteristic associated with ring methane hydrogen atoms and other peaks also [23-24].

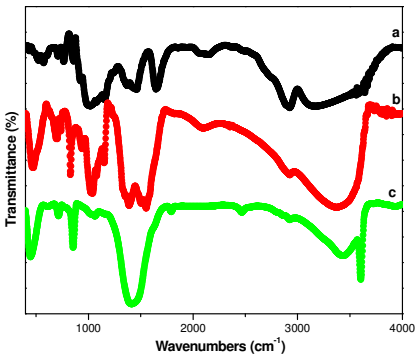

Figure 3. FTIR spectra of (a) ZnO NPs, (b) ZnO:Fe NPs and (c) capped ZnO NPs

D. UV - Optical analysis:-

Figure 4 shows the UV-absorption spectra of (a) undoped ZnO, (b) doped ZnO and (c) capped ZnO NPs. The direct band to band transition has occurred and their corresponding bandgap energy values were 3.8-3.7 eV. The capped ZnO NPs result shows a little red-shift and believed that the effect of starch encapsulation on ZnO crystal. Moreover, the absorption nature was decreased with respect to the undoped and doped ZnO NPs (indicated by down arrows). From all the nanoparticles, the bandgap value increased with decreasing particles size due to quantum confinement effect when compared with bulk ZnO crystal.

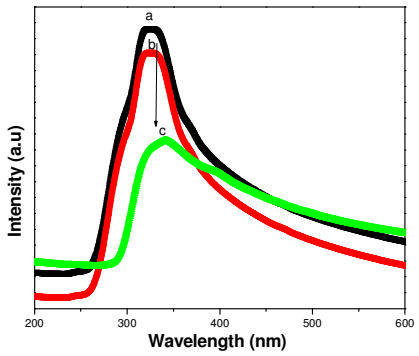

Figure 4. UV-Absorption spectra of (a) ZnO NPs, (b) ZnO:Fe NPs and (c) capped ZnO NPs

E. PL - Emission analysis:-

Figure 5 shows PL spectra of (a) undoped ZnO, (b) doped ZnO and (c) capped ZnO NPs. A rather broader near band edge emission peak appeared at 365 nm shows violet emission in addition with a strong and green emission at 550 nm. Generally without any capping agents, the ZnO particle exhibits two emissions [25]. One is relatively sharp but weak in the ultraviolet region due to the recombination of electrons and holes at the near band edges. The other is a broad and strong peak as green emission due to the existence of oxygen vacancies on the surface. Usually, the bulk material does not show this much of luminescence because of its indirect bandgap property. It is believed that whenever quantum confinement takes place their bandgap nature changes from indirect to direct bandgap [26-27]. When being direct bandgap for doped or encapsulated materials wider photoluminescence is possible. Since the ZnO visible emission originates from electrons being trapped in random surface holes, this is not from electron transitions from the conduction band to the valence band and the PL emission properties of CdSe or CdTe are better than those of ZnO nanoparticles [28].

From the Fe doped ZnO NPs, the green emission can be assigned to the transition between energy levels of Fe ions. The emission occupies blue to red region and the violet intensity is strongly quenched with the Fe ion entering into the ZnO crystal lattice (indicated by down arrows). In addition, for the red shift, it is probably due to the increasing number of PL centers of Fe element. The quenching of UV emission band could be due to the Fe ions in ZnO that act as a quencher. From the capped ZnO NPs, the small emission peak at 362 nm shows violet emission and also the maximum emission intensity peak were obtained around 440 nm with very strong (indicated by up arrows) and broad violet-blue emission band extended upto green region. By using capping agent, that is encapsulated ZnO particles show quenched green emission and enhanced blue emission due to the surface passivation of the oxygen vacancies while the green emission was disappeared. The blue-shifted emission might be attributed to the smaller particles that adhered together to form the elongated particles was reported as early [29-30]. Therefore, we conclude that, this is one of the interesting emission in ZnO nanostructures. In both samples, the violet band edge emission was obtained due to the recombination of free excitons [31]. Therefore, the nano-sized particles emission behaviors were changed and then blue shifted due to the quantum confinement effect [32-33].

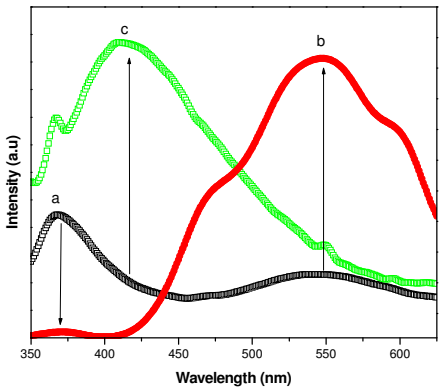

Figure 5. PL emission spectra of (a) ZnO NPs, (b) ZnO:Fe NPs and (c) capped ZnO NPs

E. Antibacterial analysis:-

The present work is focused to investigate the killing effects of NPs on *E.coli bacteria* and the method was quite similar to the previous reports [34-36]. Usually, microbial effects have changed their bacteria surface morphology when the NPs interacted with bacteria. Figure 6 shows the antibacterial activity of (a) undoped ZnO, (b) doped ZnO and (c) capped ZnO NPs, with reference samples.

The undoped and Fe doped ZnO NPs exhibits zone of inhibition and it indicates the toxic effects. The killing effect results are matched with the previous report [37]. Here, the capped ZnO NPs exhibits very less toxic effects which were related not only like the largest particles but also the aggregation of the sample.

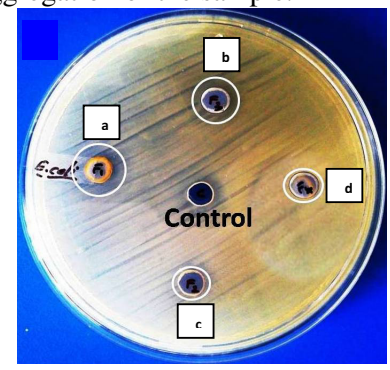

Figure 6. Antibacterial activity of (a) ZnO NPs, (b) ZnO:Fe NPs and (c)

capped ZnO NPs, and (d) reference sample

Consequently, smaller particles having the larger surface area available for interaction will give more bacterial effect than the larger particles and it was also confirmed from the previous reports [38].

IV. Conclusion:

A simple chemical precipitation method was used to prepare the undoped ZnO, doped ZnO and capped ZnO NPs. The XRD pattern results show the hexagonal crystal structure and its crystallite sizes were 15-20 nm. The TEM images indicate a spherical shaped particles nature. Since the Zn-O bonding was confirmed using FTIR technique. The UV optical spectrum shows a blue-shifted absorption band due to confinement effect. From the PL analysis, violet and simple green emissions were observed for ZnO NPs and blue emission was observed for capped ZnO NPs. Further the bacterial activity on *E.coli* is helpful to confirm and suggest that, the capped ZnO NPs is less toxic effect for living organisms as well as the ZnO NPs is suitable for antibacterial activity.

References:

[1] L. Brus, Appl. Phys. Mater. Sci. Process 53 (1991), 465-474.

[2] C.B. Murray, D.J. Norris, M.G. Bawendi, J. Am. Chem. Soc., 115 (1993), 8706-8715.

[3] A.P. Alivisatos, Science 271 (1996), 933-937.

[4] X. Michalet, F.F. Pinaud, L.A. Bentolila, J.M. Tsay, S. Doose, J.J. Li, G. Sundaresan, A.M. Wu, S.S. Gambhir, S. Weiss, Science 307 (2005), 538-544.

[5] C.B. Murray, C.R. Kagan, M.G. Bawendi, Annu. Rev. Mater. Sci., 30 (2000), 545-610.

[6] M. Li, H. Bala, X. Lv, X. Ma, F. Sun, L. Tang, Z. Wang, Mater. Lett., 61 (2007), 690-693.

[7] A. Ratkovich, R.L. Penn, Mat. Res. Bul., 44 (2009), 993-998.

[8] Y.L. Wu, A.I.Y. Tok, X.T. Zeng, C.S. Lim, L.C. Kwek and F.C.Y. Bocy, Nanotech., 19 (2008), 345605 (9 pp).

[9] P. Raveendran, J. Fua and L. Scott, Chem., 8 (2006), 34-38.

[10] C. Engelbrekt, K. H. Sorensen, J. Zhang, A.C. Welinder, P.S. Jensen and J. Ulstrup, J. Mater. Chem., 19 (2009), 7839-7847.

[11] Q.G. Wei, S.Z. Kang and J. Mu, Colloid. Surf. A., 247A (2004), 125-127.

[12] L.K. Adams, D.Y. Lyon, P.J.J. Alvarez, Water Res., 40 (2006), 3527-3532.

[13] Q. Wei, S.Z. Kang, J. Mu, Colloid. Surf. A: Physicochem. Eng. Aspects 247 (2004) 125-127.

[14] J.H. Li, C. L. Ren, X.Y. Liu, Z.D. Hu, D.S. Xue, Mater. Sci. Engg., A 458 (2007) 319-322.

[15] K.M. Reddy, K. Feris, J. Bell, D.G. Wingett, C. Hanley, A. Punnoose, Appl. Phys. Lett., 90 (2007), 213902 (3 pp).

[16] Y. Xie, Y. He, P.L. Irwin, T. Jin and X. Shi, Appl. Environ. Microbiol., 77 (2011), 2325-2331.

[17] A. Lipovsky, Y. Nitzan, A. Gedanken and R. Lubart, Nanotech., 22 (2011), 105101 (5 pp).

[18] G. Applerot, A. Lipovsky, R. Dror, N. Perkas, Y. Nitzan, R. Lubart and A.

Gedanken, Adv. Funct. Mater., 19 (2009), 842-852.

[19] N. Padmavathy, R. Vijayaraghavan, Sci. Tech. Adv. Mater., 9 (2008), 035004 (7 pp).

[20] L. Zhang, Y. Jiang, Y. Ding, M. Povey and D. York, J. Nanopart. Res., 9 (2007), 479-489.

[21] Z. Huang, X. Zheng, D. Yan, G. Yin, X. Liao, Y. Kang, Y. Yao, D. Huang and B. Hao, Langmuir 24 (2008), 4140-4144.

[22] O. S. Oluwafemi, Colloid. Surf. B: Biointer., 73 (2009), 382-386

[23] Jiang Z, Huang Z, Yang P, Chen J, Xin Y, Xu, J Compos. Sci. Technol. 68 (2008), 3240-3244.

[24] Zamari R, Zakaria A, Ahangar HA, Darroudi M, Zak A and Drummen GPC, J. Alloys Compound., 516 (2012), 41-48.

[25] D. Sun, H.J. Sue and N. Miyatake, J. Phys. Chem., 112 (2008), 16002-16010.

[26] A. van Dijken, E. A. Meulenkamp, D. Vanmaekelbergh and A. Meijerink, J. Lumin., 454 (2000) 87-89.

[27] L. Poul, N. Jouini, F. Fievet, Chem. Mater., 12 (2000), 3123-3132.
[28] Oluwatobi S. Oluwafemi, Colloid. Surf. B: Biointer., 73 (2009), 382-386.

[29] N. Vigneshwaran, S. Kumar, A.A. Kathe, P.V. Varadarajan and V. Prasad, Nanotech., 17 (2006) 5087-5095.

[30] F. Xu, Z.Y. Yuan, G.H. Du, T.Z. Ren, C. Bouvy, M. Halasa and B.L. Su, Nanotech., 17 (2006), 588-594.

[31] S. Chandramouleeswaran, S.T. Mhaske, A.A. Kathe, P.V. Varadarajan, V. Prasad and N. Vigneshwaran, Nanotech., 18 (2007) 385702-385710.

[32] J. Yang, J. Lang, L. Yang, Y. Zhang, D. Wang, H. Fan, H. Liu, Y. Wang and M. Gao, J. Alloys and Comp., 450 (2008), 521-524.

[33] S. Makhluf, R. Dror, Y. Nitzan, Y. Abramovich, R. Jelinek, A. Gedanken, Adv. Funct. Mater., 17 (2005), 1708-1715.

[34] Z. Lu, C. M. Li, H. Bao, Y. Qiao, Y. Toh, X. Yang, Langmuir 24 (2008), 5445-5452.

[35] R. Wahab, Y. S. Kim, A. Mishra, S-II. Yun, H. S. Shin, Nanoscale Res. Lett., 5 (2010), 1675-1681.

[36] R. B. Zhao, D. L. Hou, J.M. Guo, C. M. Zhen, G. D. Tang, J. Supercond. Nov. Magn., 23 (2010), 1261-1265.

[37] P. J. Rivero, A. Urrutia, J. Goicoechea, C. R. Zamarreno, F. J. Arregui and I. R. Matias, Nanoscale Res. Lett., 6 (2011), 305 (7 pp).

[38] C. Dong, D. Song, J. Cairney, O. L. Maddan, G. He, Y. Deng, Mater. Res. Bul., 46 (2011), 576-582.